Prepared for submission to JHEP MS-TP-14-02

Nuclear parton density modifications from low-mass lepton pair production at the LHC

M. Brandt, M. Klasen, F. König

Institut für Theoretische Physik, Westfälische Wilhelms-Universität Münster, Wilhelm-Klemm-Straße 9, D-48149 Münster, Germany

E-mail: matthiasbrandt@uni-muenster.de, michael.klasen@uni-muenster.de, f.koenig@uni-muenster.de

Abstract: In this article, we investigate the potential of low-mass lepton pair production in proton-ion collisions at the LHC to constrain nuclear modifications of parton densities. Similarly to prompt photon production, the transverse momentum spectrum is shown to be dominated by the QCD Compton process, but has virtually no fragmentation or isolation uncertainties. Depending on the orientation of the proton and ion beams and on the use of central or forward detector components, all interesting regions of nuclear effects (shadowing, antishadowing, isospin and EMC effects) can be probed. Ratios of cross sections allow to eliminate theoretical scale and bare-proton parton density errors as well as many experimental systematic uncertainties.

arXiv:1401.6817v1 [hep-ph] 27 Jan 2014

Contents

1 **Introduction** 1

2 **Nuclear parton density uncertainties** 2

3 **Partonic subprocesses in proton-ion collisions** 5

4 **Low-mass lepton pair production at the LHC** 10

5 **Conclusions** 14

1 Introduction

An important physics goal of the Large Hadron Collider (LHC) program at CERN is the study of the quark-gluon plasma, a deconfined state of matter created at high temperatures in heavy-ion collisions. For an unambiguous identification of its properties, e.g. through thermal radiation of photons with small transverse momenta [1], a subtraction of cold nuclear effects is mandatory [2]. In particular, the parton density functions (PDFs) in nucleons are significantly modified when the latter do not collide freely, but are bound in nuclear states [3–6], and this must properly be taken into account [7].

Unfortunately, nuclear PDFs are known with much less precision than free proton PDFs. Both are mainly determined in deep-inelastic scattering (DIS), but for nuclei only fixed-target data with a very restricted range in Bjorken-x and photon virtuality Q^2 are available. Since DIS is mainly sensitive to the (valence) quark density, it is supplemented by measurements of Drell-Yan lepton-pair production (again in fixed-target experiments), which helps to constrain the antiquark densities and also the quark densities with a different weighting than the DIS data [3, 4]. More recently, data on neutral [5, 6] and charged [6] pion production in proton-ion collisions at BNL's Relativistic Heavy Ion Collider (RHIC) have been added in order to put first direct constraints on the poorly known gluon density.

It is well known that the gluon density in protons and nuclei can also be constrained with prompt photon production in hadronic collisions. In particular, it has been proposed to use RHIC and LHC data on photons with low transverse momenta produced in pA collisions to measure the shadowing effects in the low-x region [8]. At higher transverse momenta, this process can also become sensitive to antishadowing and the EMC effect, albeit not the Fermi motion [9]. However, photons coming from pion decay must be eliminated, e.g. by applying an isolation criterion [10], and the contribution of quark and gluon fragmentation to photons must be parametrised [11], which induces considerable uncertainties.

In this paper we advocate that these difficulties can be avoided by the use of virtual photons, which have neither decay nor fragmentation contributions and need not be isolated

from hadronic spectators, since they give rise to an experimentally well identifiable lepton (electron or muon) pair. This idea was first introduced for unpolarised [12] and polarised [13] pp collisions, recently extended to weak boson production at very large transverse momenta [14], and is now applied to pA collisions. The transverse momentum spectra of massive vector bosons (J/Ψ, Υ and W/Z) produced in pA collisions have recently been studied elsewhere [15, 16]. At variance with the Drell-Yan process, which is dominated at low transverse momenta by quark-antiquark annihilation, we show that, in the region of low virtuality and high transverse momentum of the lepton pair, its production in pA collisions is dominated, just like the production of prompt photons, by quark-gluon scattering and is thus very sensitive to the poorly constrained nuclear modification of the gluon PDF. We also demonstrate that other uncertainties like those from scale variations and the free gluon PDFs largely cancel out in ratios of cross sections and thus do not spoil this sensitivity.

The remainder of the paper is organised as follows: In Sec. 2, we review the current uncertainties on nuclear PDFs, and in Sec. 3 we establish numerically the dominance of quark-gluon scattering. Sec. 4 contains our main results for low-mass lepton pair production at the LHC and examines its sensitivity to various nuclear modification effects. Our conclusions are presented in Sec. 5.

2 Nuclear parton density uncertainties

First, we review in this section the current level of uncertainty in the distribution of a parton i in a nucleus A, $f_{i/A}(x,\mu_f)$, which depends on the longitudinal momentum fraction x carried by the parton and the factorisation scale μ_f. As we will be mostly interested in ratios of cross sections in pA over those in pp collisions, we focus on the uncertainty of the so-called nuclear modification factor

$$R_{i/A}(x,\mu_f) = \frac{f_{i/A}(x,\mu_f)}{f_{i/p}(x,\mu_f)} \tag{2.1}$$

rather than the intrinsic uncertainties of the bare proton PDFs $f_{i/p}(x,\mu_f)$, which should cancel to a large extent in ratios of cross sections. A modification factor as in Eq. (2.1) is also usually employed in global fits of nuclear PDFs to parametrise nuclear modification effects, the notable exception being the one performed by the nCTEQ collaboration [4]. Cross section ratios will later of course be computed taking the convolution of partonic cross sections with different PDFs into account.

In this paper, we use the EPS09 nuclear PDFs as our baseline [5], which are based on the factorised ansatz in Eq. (2.1) and CTEQ6.1M [17] free-proton PDFs. The bound-neutron PDFs are then obtained by assuming isospin symmetry. E.g. the total up-quark (u) distribution per nucleon in a nucleus A with Z protons is

$$f_{u/A}(x,\mu_f) = \frac{Z}{A}[R^v_{u/A} f^v_{u/p} + R^s_{u/A} f^s_{u/p}] + \frac{A-Z}{A}[R^v_{d/A} f^v_{d/p} + R^s_{d/A} f^s_{d/p}], \tag{2.2}$$

where d corresponds to the down-quark and the superscripts v and s refer to valence and sea quark contributions, respectively. The parametrisation of the nuclear modifications

$R_{i/A}(x,\mu_f)$ is performed at the charm quark mass (m_c) threshold imposing the momentum and baryon number sum rules

$$\sum_{i=q,\overline{q},g}\int_0^1 dx\, x f_{i/A}(x,m_c)=1, \quad \int_0^1 dx\left[f^v_{u/A}(x,m_c)+f^v_{d/A}(x,m_c)\right]=3, \tag{2.3}$$

for each nucleus A separately. At higher scales, the nuclear PDFs are obtained by solving the DGLAP evolution equations. This approach results in an excellent fit to the different types of nuclear hard-process data [5], suggesting that factorisation works well in the energy range studied and that the extracted nuclear PDFs are universal in the region $x \geq 0.005$, $\mu_f \geq 1.3$ GeV.

In addition to the theoretical uncertainties of the free-proton PDFs, obtained using the 40 error sets of the CTEQ6.1M parametrisation [17], 30 error sets are assigned pairwise to the uncorrelated eigendirections of the 15 parameters fitted to the nuclear collision data sets. A total uncertainty band at 90% confidence level is then calculated from the 71 sets defined by fixing either $R_{i/A}(x,\mu_f)$ to the best fit value and varying the free-proton PDFs or fixing the latter to its best fit value and varying the former. These variations then contribute pairwise to the size of the upper and lower errors via

$$\delta^+ f = \sqrt{\sum_i [\max(f_i^{(+)}-f_0, f_i^{(-)}-f_0, 0)]^2}, \tag{2.4}$$

$$\delta^- f = \sqrt{\sum_i [\max(f_0-f_i^{(+)}, f_0-f_i^{(-)}, 0)]^2}. \tag{2.5}$$

As the authors acknowledge, this factorised approach represents a simplification, violating, e.g., in some cases momentum conservation, so that strictly speaking the free- and bound-proton PDF uncertainty analyses should not be separated [5].

In order to estimate the bias from different underlying free-proton PDFs, parametrisations of the nuclear modification, and fitted nuclear data sets, we also study the best fits of the HKN07 [3], nCTEQ [4] and DSSZ [6] collaborations. In particular, the HKN07 nuclear PDFs are based on the MRST1998 free-proton set [18] and those of DSSZ on the more recent MSTW2008 set [19]. The nCTEQ parametrisation is (so far) the only one that does not rely on a factorisation into a nuclear modification factor and free-proton PDFs. Instead it introduces an explicit A-dependence in the coefficients of the x-dependent functional form of the PDFs at the starting scale. Only the technical framework of the CTEQ6M analysis is used here [20].

Since the uncertainties on the free proton PDFs cancel out to a large extent in ratios of cross sections, we plot in Fig. 1 only the nuclear modification factor defined in Eq. (2.1) for protons bound in lead ions and as obtained in the central EPS09 fit (full) with its 30 error sets related to the nuclear uncertainty (yellow band) [5], in the HKN07 (dashed) [3], nCTEQ (dot-dashed) [4] and DSSZ (dotted) [6] fits. Error bands are only shown for the EPS09 analysis. From left to right, the up-quark, strange-quark and gluon densities are shown separately for $\mu_f = 50$ GeV (top) and 500 GeV (bottom) pertinent to the transverse momenta of lepton pairs that we will study later.

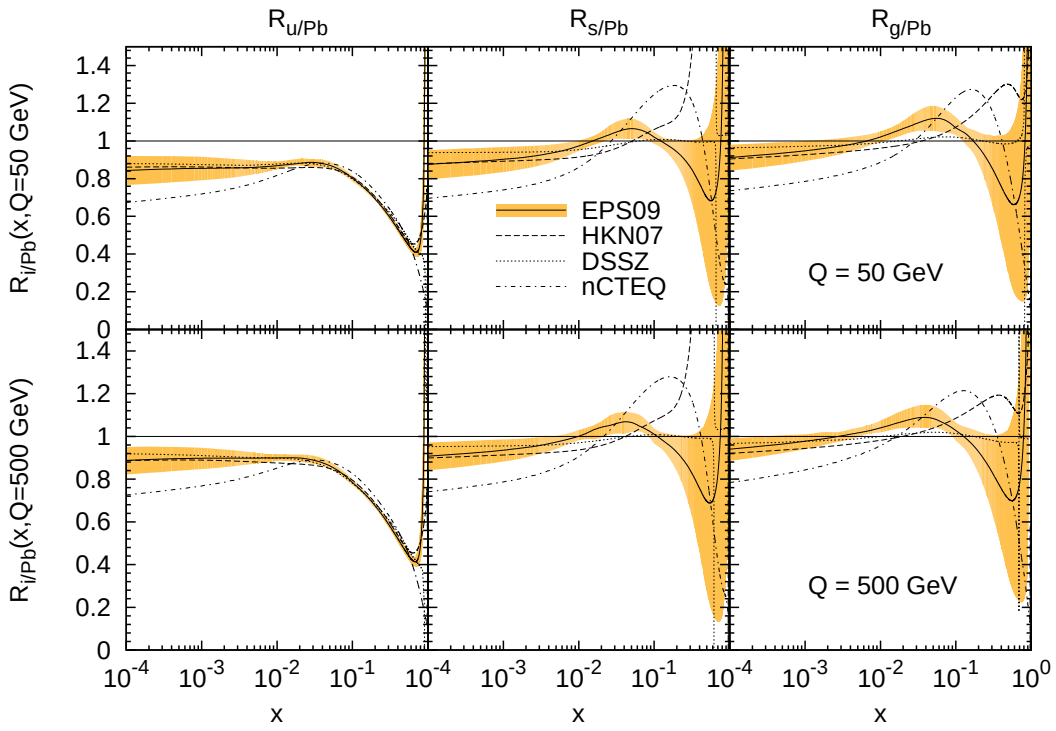

Figure 1. Modifications of up-quark (left), strange-quark (centre) and gluon (right) PDFs in lead nuclei with respect to bare proton PDFs at the factorisation scales 50 GeV (top) and 500 GeV (bottom) and as obtained in global fits by four different groups.

All four fits agree reasonably well with respect to the nuclear modification of the up-quark density, which is dominated by valence quarks and thus mostly modified by strong isospin effects at large x. Qualitatively, the shadowing and antishadowing regions below and above $x \sim 10^{-2}$ as well as the EMC effect and Fermi motion regions above $x \sim 0.1$ and 0.8 are also similar in all distributions. However, the four fits disagree not only about their sizes, which vary from 10 to 30 % in the shadowing and antishadowing regions and from 0 to 80% in the region of the EMC effect, but they also disagree about the relevant x-regions. Only the valence-dominated up-quark distribution at intermediate x is well constrained by the DIS data used in all fits. Furthermore, the EPS09 parametrisation clearly underestimates the true uncertainty, as the three other curves often fall outside its band width. This is particularly true for the nCTEQ parametrisation, which is obtained without a factorised fit and has more free parameters than the factorised ansatz of EPS09. A comparison of Fig. 1 with Fig. 3 in Ref. [5] exhibits that the uncertainties on these effects decrease when the factorisation scale is increased from 1.3 GeV and 10 GeV as shown there to 50 and 500 GeV as shown here, but only in the low-x region. This can be traced back to the constraints imposed by the QCD evolution equations. Note, however, that the large uncertainties at high x persist, in particular for the gluon and the sea-dominated strange quark, where DSSZ, e.g., predict much smaller nuclear modifications than the other groups.

New experimental information has recently become available from charged particle

production at the LHC, where the CMS collaboration measure antishadowing enhancements of up to $40 \pm 20\%$ at values of $x = 0.01 \ldots 0.05$, i.e. much more than predicted by the EPS09 and even nCTEQ parametrisations [21].

3 Partonic subprocesses in proton-ion collisions

We now establish in this section which partonic subprocesses contribute to the production of low-mass lepton pairs at the LHC in different regions of the transverse momentum (p_T) of the pair. This will later allow us to estimate the sensitivity of the corresponding experimental measurements on the nuclear modification effects for quarks and gluons, respectively. To this end, we compute the transverse momentum spectra of electron-positron and muon pairs produced in proton-lead collisions at a centre-of-mass energy of $\sqrt{s} = 5.02$ TeV, that has recently been reached at the LHC.

The sensitivities of the ALICE, ATLAS and CMS experiments to continuum production of lepton pairs in pp collisions have in 2011 allowed to reach transverse momenta up to 100 GeV and might in the future extend up to 1000 GeV [22]. In these regions, we can rely on a next-to-leading order (NLO) calculation, and resummation effects at low transverse momenta need not be taken into account [12]. With the ALICE detector, electron and muon pairs are measured in the pp centre-of-mass frame at rapidities of $|\eta| < 0.9$ [23] and $2.5 < \eta < 4$ [24], respectively. In pA collisions, these regions are shifted by a boost of $\Delta\eta = 0.465$ in the direction of the proton beam due to the energy asymmetry of the LHC beams ($E_p = 4$ TeV, $E_{\mathrm{Pb}} = 1.58 \cdot A$ TeV) [25]. In order to avoid the J/Ψ and Υ resonance regions, we consider invariant lepton masses of $2m_\mu < Q < 2.5$ GeV and 5 GeV $< Q <$ 6 GeV. The inner detectors of the ATLAS [26] and CMS [27] experiments allow to measure muons with rapidities $|\eta| < 2.4$ in the centre-of-mass frame. The range for electrons is often adjusted for comparability of the two channels. As a typical invariant mass range, we will employ here 12 GeV $< Q <$ 25 GeV.

Total cross sections for central and forward lepton-pair production in proton-lead collisions at the LHC with a centre-of-mass energy of $\sqrt{s} = 5.02$ TeV are shown in Fig. 2. In the 2013 proton-lead run, a total luminosity of only about 32 nb^{-1} has been delivered, while in the 2013 reference pp run at the same energy a total luminosity of 5.38 pb^{-1} has been reached. With this luminosity, centrally produced low-mass electron pairs can be measured with transverse momenta of up to 50 GeV (full line). For larger invariant masses (dashed line) or muons in the forward ALICE detector (dotted and dot-dashed lines), the cross sections are lower by up to an order of magnitude. In principle, much higher luminosities can of course be achieved at the LHC, as has been demonstrated by the 2012 pp run with an integrated of 23.3 fb^{-1}, but for meaningful studies of cold nuclear effects, it would be necessary to allocate sufficient beam time to proton-lead collisions.

At leading order (LO) of perturbative QCD, the production of lepton pairs with finite transverse momentum proceeds through the fusion process $q\bar{q} \to \gamma^* g$ and through the so-called QCD Compton process $qg \to \gamma^* q$, where in both cases the virtual photon decays into a lepton pair. While at low transverse momenta the former process is expected to dominate and must eventually be matched to the Drell-Yan process $q\bar{q} \to \gamma^*$ with vanishing transverse

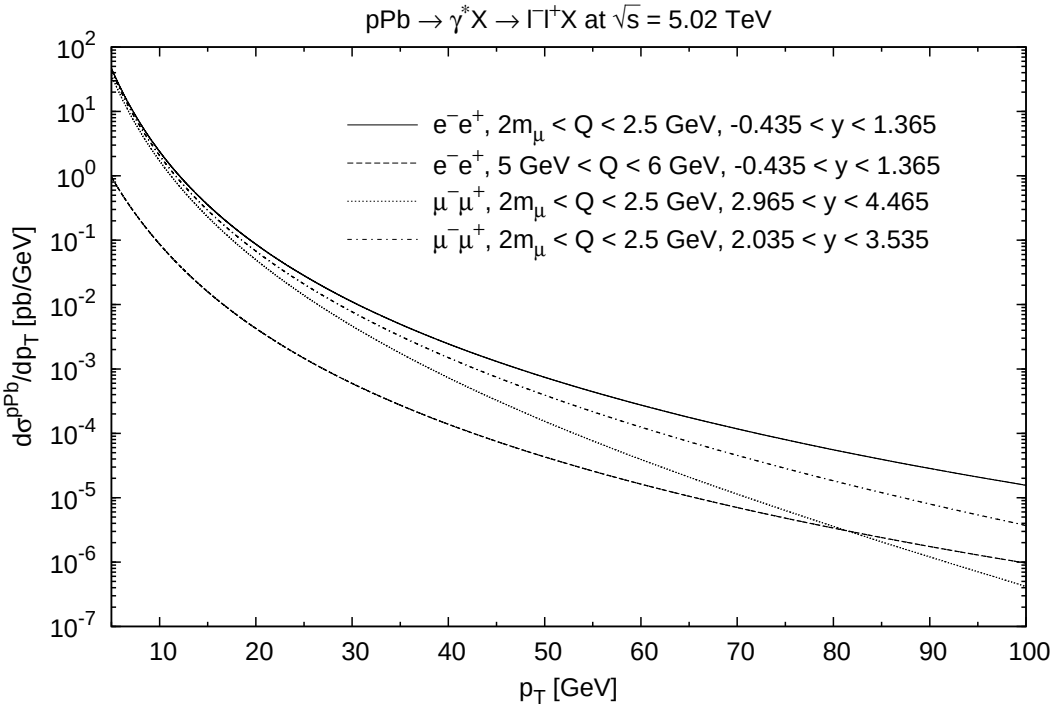
pPb → γ*X → l⁻l⁺X at √s = 5.02 TeV
e⁻e⁺, 2m_μ < Q < 2.5 GeV, -0.435 < y < 1.365
e⁻e⁺, 5 GeV < Q < 6 GeV, -0.435 < y < 1.365
μ⁻μ⁺, 2m_μ < Q < 2.5 GeV, 2.965 < y < 4.465
μ⁻μ⁺, 2m_μ < Q < 2.5 GeV, 2.035 < y < 3.535
dσ^pPb/dp_T [pb/GeV]
p_T [GeV]

Figure 2. Total cross sections for central and forward lepton-pair production in proton-lead (full, dashed and dotted lines) and lead-proton (dot-dashed line) collisions.

momentum, the latter process is expected to take over as the transverse momentum of the photon becomes larger, since this also happens for real photons.

In Fig. 3, we show the NLO fractional contributions of the quark-gluon (dashed) and quark-antiquark (dotted) processes to the inclusive central production of electron-positron pairs with invariant mass $2m_\mu < Q < 2.5$ GeV (top) and 5 GeV $< Q <$ 6 GeV (bottom) in proton-lead collisions at the LHC with a centre-of-mass energy of $\sqrt{s} = 5.02$ TeV. Processes like $qq \to \gamma^* qq$ entering only at NLO are small and not shown. For the nuclear PDFs, we have employed the central set of EPS09. As it can be seen, the QCD Compton process takes over very quickly, contributing more than 80% (top) and even more than 95% (bottom) already at small, but finite values of p_T. From the upper x-axes of these plots, we learn that the momentum fractions of the bound nucleons probed with $p_T < 100$ GeV, estimated by $x_T = 2p_T/\sqrt{s}$, lie in the range 0.002 to 0.04, i.e. in the shadowing and antishadowing regions (cf. Fig. 1). The true x-values probed in the lead ion, travelling here in the negative z-direction, are somewhat smaller ($x_{\rm Pb}/x_T = e^{-0.465} \simeq 0.63$) due to the asymmetry of the beam energies.

In Fig. 4, similar results are shown for muons produced in the forward region of the ALICE experiment. As in Fig. 3 (top), the virtuality of the photon lies just above the threshold for muon pair production, and QCD Compton scattering dominates again at the level of more than 80%. However, the asymmetry introduced by the acceptance of the muon spectrometer is now substantial, so that the x-values probed in the lead ion depend strongly

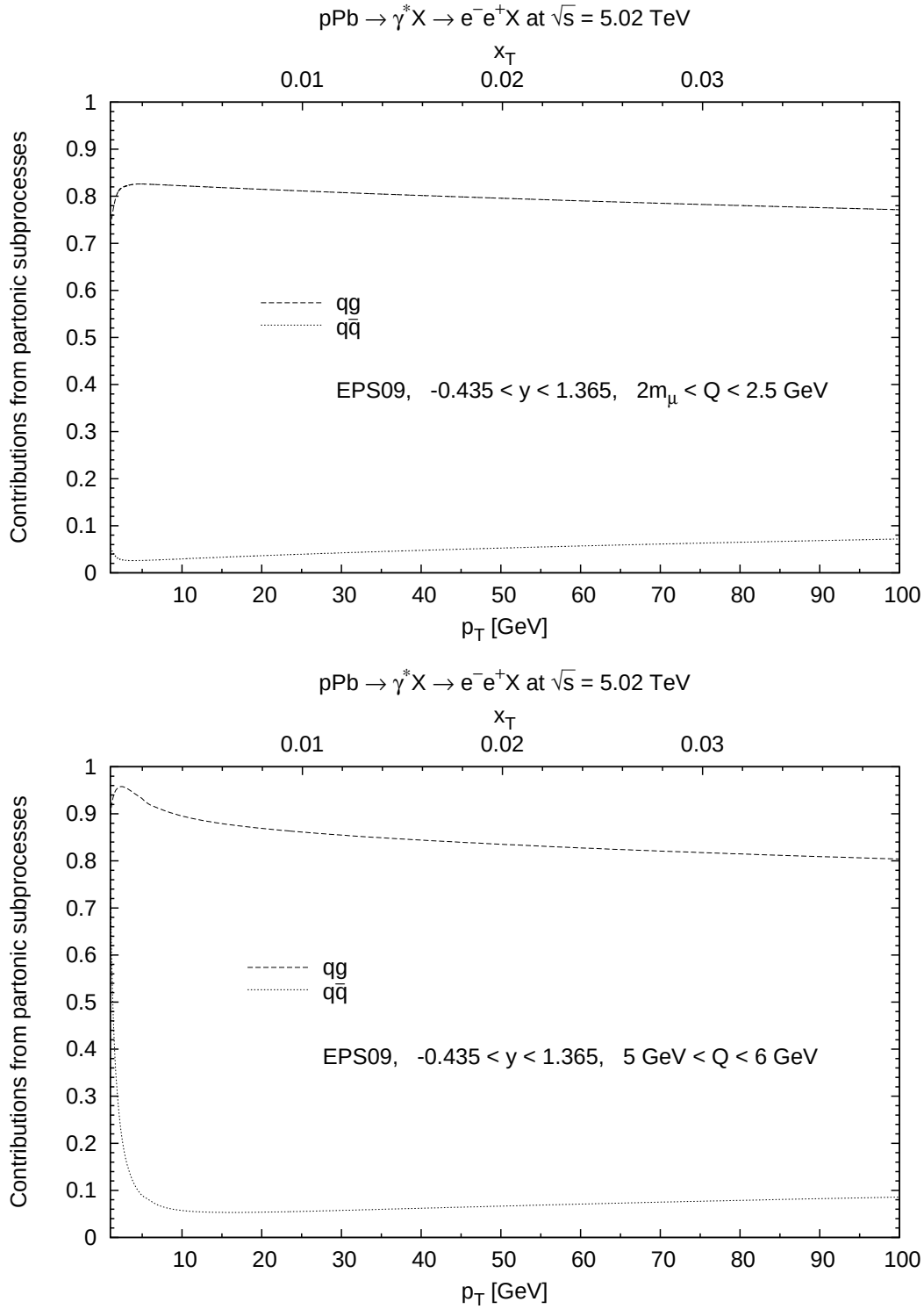

Figure 3. Fractional contributions of partonic subprocesses to low (top) and intermediate (bottom) mass electron-positron pair production at central rapidity and $p_T < 100$ GeV.

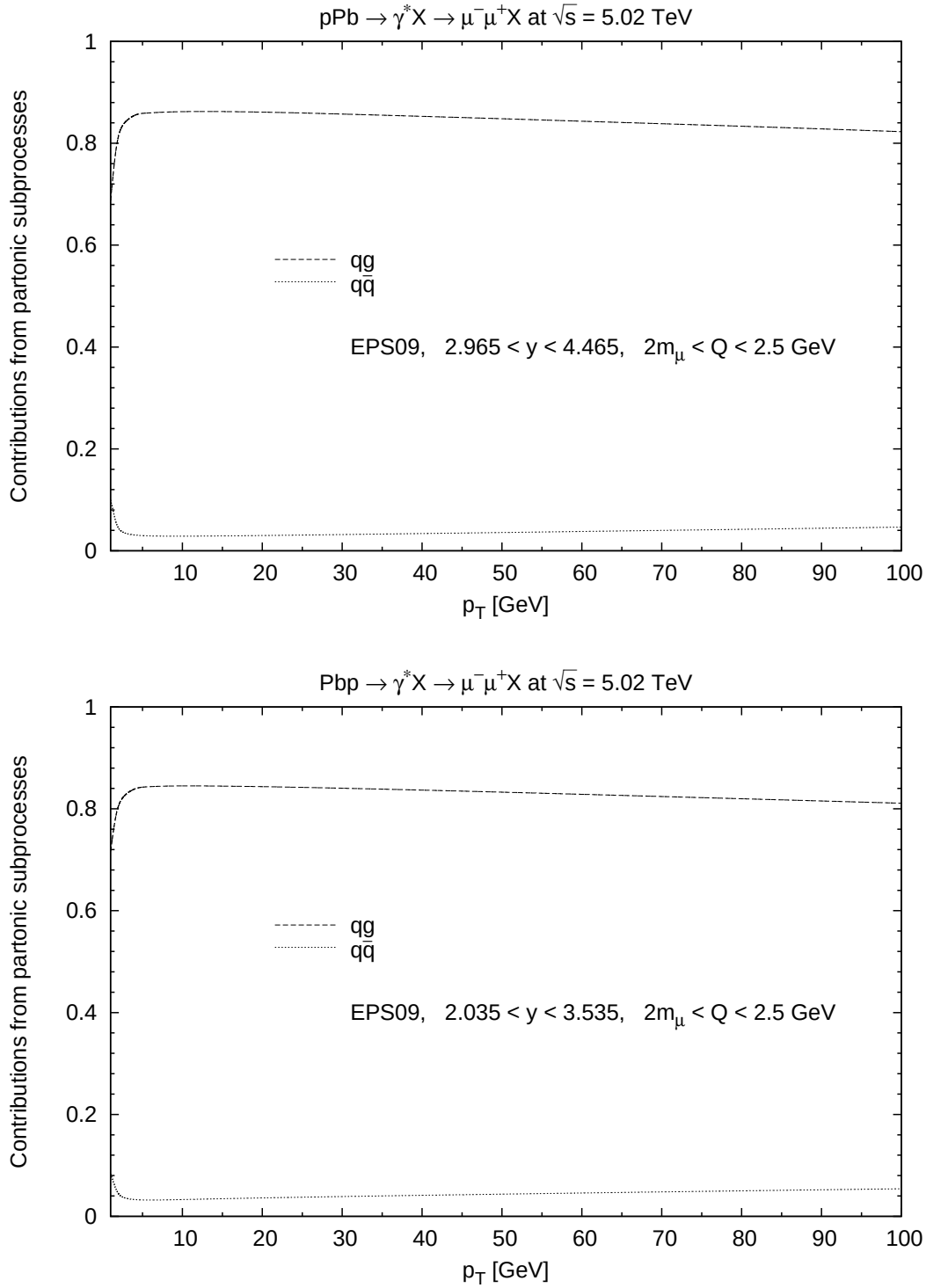
pPb → γ*X → μ⁻μ⁺X at √s = 5.02 TeV
Contributions from partonic subprocesses
qg
qq̄
EPS09, 2.965 < y < 4.465, 2m_μ < Q < 2.5 GeV
p_T [GeV]
Pbp → γ*X → μ⁻μ⁺X at √s = 5.02 TeV
Contributions from partonic subprocesses
qg
qq̄
EPS09, 2.035 < y < 3.535, 2m_μ < Q < 2.5 GeV
p_T [GeV]

Figure 4. Fractional contributions of partonic subprocesses to low-mass muon pair production at forward rapidity and $p_T < 100$ GeV in proton-lead (top) and lead-proton (bottom) collisions.

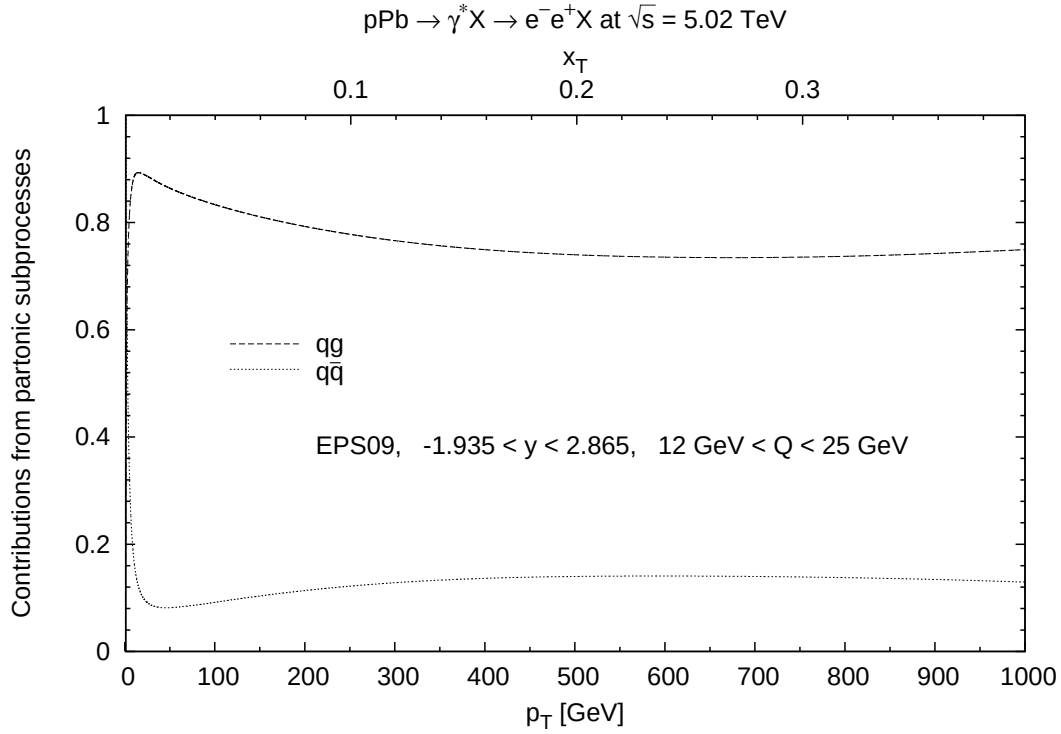

Figure 5. Fractional contributions of partonic subprocesses to intermediate-mass electron-positron pair production at central rapidity and $p_T < 1000$ GeV.

on the orientation of the muon beam. Taking the central values of x_T and muon acceptance, we find for lead ions circulating in the negative z-direction, Fig. 4 (top), $x_{\rm Pb} \simeq 0.02 \cdot e^{-3.75} \simeq 4 \cdot 10^{-4}$, so that we are here firmly in the shadowing region. For lead ions circulating in the positive z-direction, Fig. 4 (bottom), the overall dominance of QCD Compton scattering changes very little, since the asymmetry due to the beam energies is subdominant compared to the one introduced by the ALICE muon spectrometer. However, we are now probing mostly (valence) quarks in the lead ion with gluons from the proton, so that isospin effects will become very important. Furthermore, we find $x_{\rm Pb} \simeq 0.02 \cdot e^{2.75} \simeq 0.3$, so that we are here also in the region of the EMC effect.

In Fig. 5, we study the fractional contributions of partonic subprocesses in the ATLAS and CMS experiments with larger electron and muon acceptance at central rapidity $|\eta| < 2.4$ and a larger transverse momentum range $p_T < 1000$ GeV, but requiring also a larger invariant mass of the lepton pair, e.g. 12 GeV $< Q <$ 25 GeV. For these photon virtualities, the dominance of QCD Compton scattering is a bit smaller than for the region between the J/Ψ and Υ resonances shown in Fig. 3 (bottom), but still substantial with more than 70% in the complete p_T-range. With ATLAS and CMS, larger x_T-values of 0.01 to 0.4 could be probed, where the true $x_{\rm Pb}$ values depend in addition on the beam direction and possible additional experimental rapidity cuts, but where we are mostly in the regions of isospin and EMC effects.

4 Low-mass lepton pair production at the LHC

In the previous section, we have established the dominance of the QCD Compton scattering process over quark-antiquark annihilation for low-mass lepton pair production in proton-lead collisions at the LHC. We have also determined the kinematic regions where the ALICE, ATLAS and CMS experiments are expected to be sensitive to shadowing, antishadowing, EMC and isospin effects that modify the gluon and quark distributions of bound nucleons.

We can therefore now study numerically, at NLO QCD, the level of uncertainty present in the current parametrisations of nuclear PDFs in the transverse momentum distributions of lepton pairs in order to determine the potential for their reduction with the corresponding measurements at the LHC. We will do this through ratios of differential cross sections

$$R^{\mathrm{pPb}} = \frac{\mathrm{d}\sigma^{\mathrm{pPb}}/\mathrm{d}p_T}{\mathrm{d}\sigma^{\mathrm{pp}}/\mathrm{d}p_T}, \tag{4.1}$$

where theoretical uncertainties, in particular those coming from variations of the unphysical renormalization and bare-proton factorisation scales and of the parametrisation of the bare-proton PDFs, are expected to cancel out to a large extent. However, the nuclear modification factor may still show some residual factorisation scale dependence. We stress again that our numerical results have been obtained taking the full convolution of partonic cross sections and PDFs in the numerator and denominator into account.

In Fig. 6 (top), this ratio is shown for the acceptance of the central ALICE detector and various nuclear PDF parametrisations. Apart from the central EPS09 prediction (full), we show its associated uncertainty band (yellow). As expected, the intermediate x-range from 0.002 to 0.04 corresponds to the transition from the shadowing to the antishadowing regions, where the valence quarks are relatively well determined (cf. Fig. 1) and the overall uncertainty is estimated by EPS09 to be relatively small, i.e. $\pm 6\%$ at small and 2.5% at larger p_T. Luckily, the residual scale dependence (red), when the scales are varied simultaneously in the numerator and denominator, is even smaller by about a factor of two at small p_T, and it is practically absent at larger p_T. However, one should not forget the theoretical bias and restricted data set entering each global nuclear PDF parametrisation. It is indeed instructive to see that the older HKN07 parametrisation (dashed), but also the very recent DSSZ parametrisations fall outside the EPS09 uncertainty band, differing quantitatively by up to 8% and qualitatively even about the nature of the nuclear effects in this x-region. The discrepancy is even more striking for the nCTEQ parametrisation, which is obtained without a factorised ansatz and differs by up to 16% from the central EPS09 prediction at low p_T. We also observe that isospin effects (green) play no role here, since we are in a sea- and gluon-dominated regime. The situation is very similar if we slightly increase in Fig. 6 (bottom) the virtuality of the produced photon, so that it falls between the J/Ψ and Υ resonances.

With the ALICE muon spectrometer at forward rapidities, substantially smaller x-values in the bound nucleons are probed, so that we are moving more into the shadowing region. This is confirmed by Fig. 7 (top). The EPS09 uncertainty now reaches $\pm 9\%$ at low p_T. The residual scale uncertainty there is again much smaller (up to 2%), so that LHC

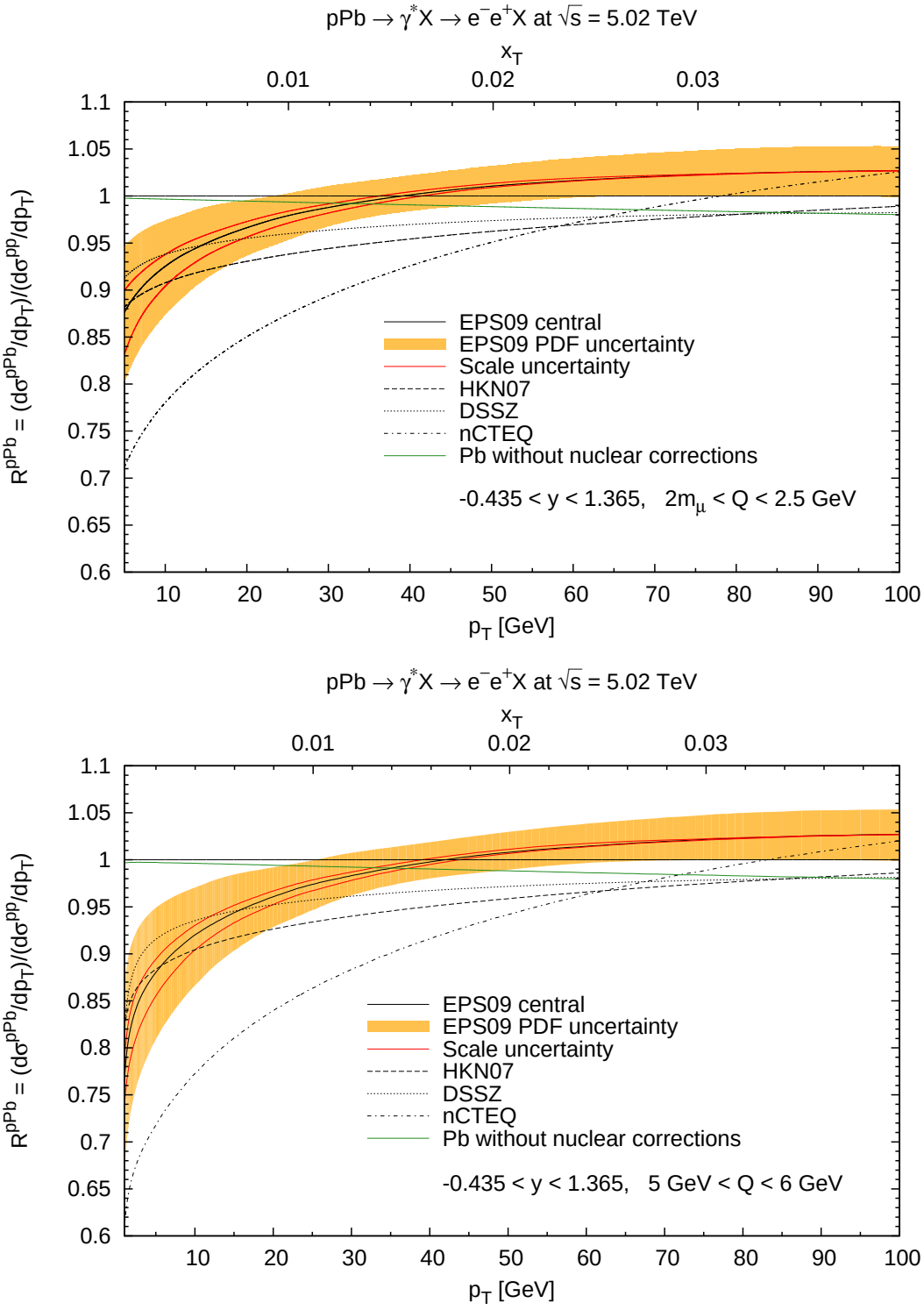

Figure 6. Ratios of transverse-momentum distributions of low (top) and intermediate (bottom) mass electron-positron pairs produced centrally in proton-lead and proton-proton collisions as predicted from various nuclear PDF parametrisations.

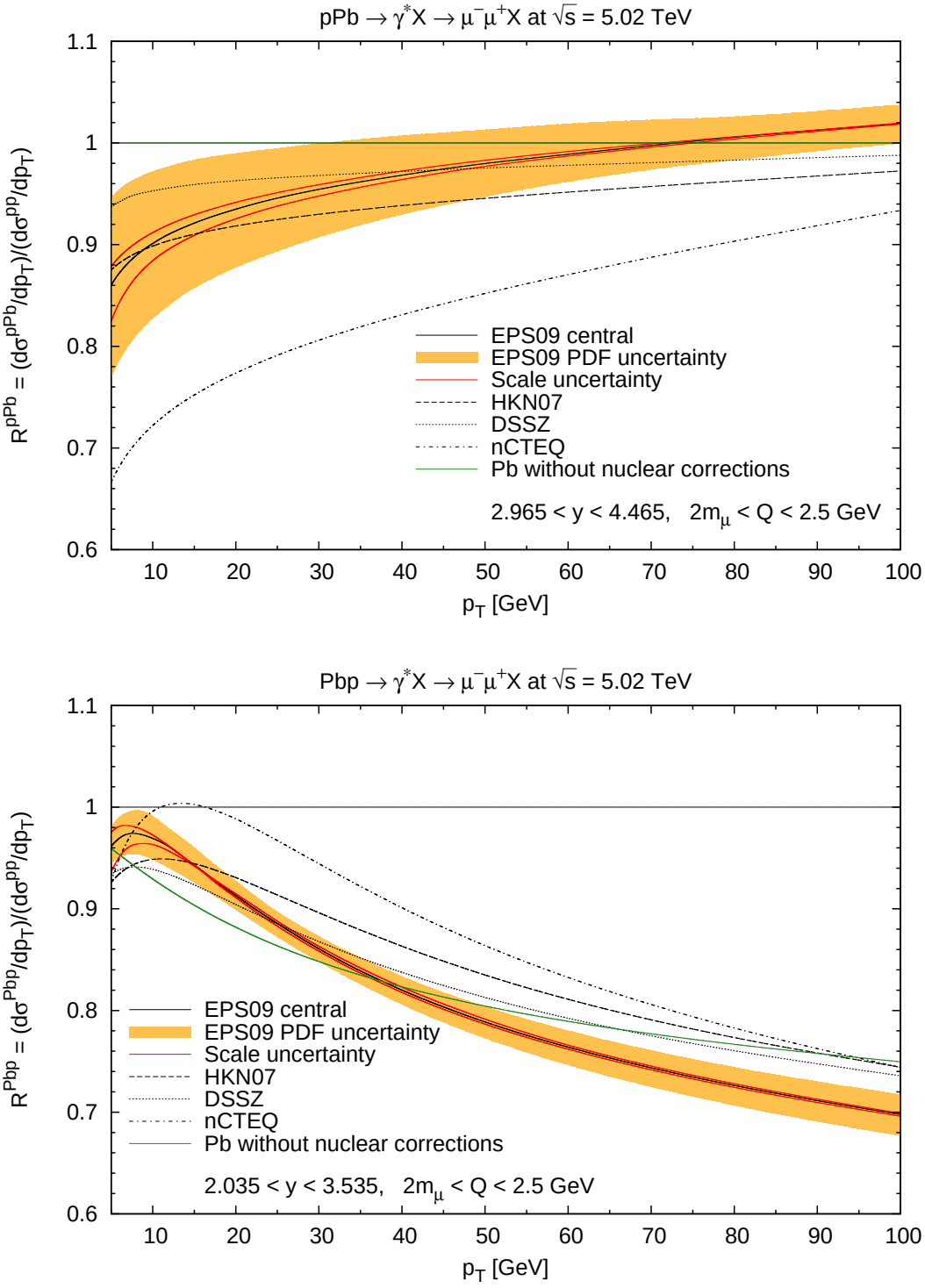

Figure 7. Ratios of transverse-momentum distributions of forward muon pairs produced in proton-lead (top) / lead-proton (bottom) and proton-proton collisions as predicted from various nuclear PDF parametrisations.

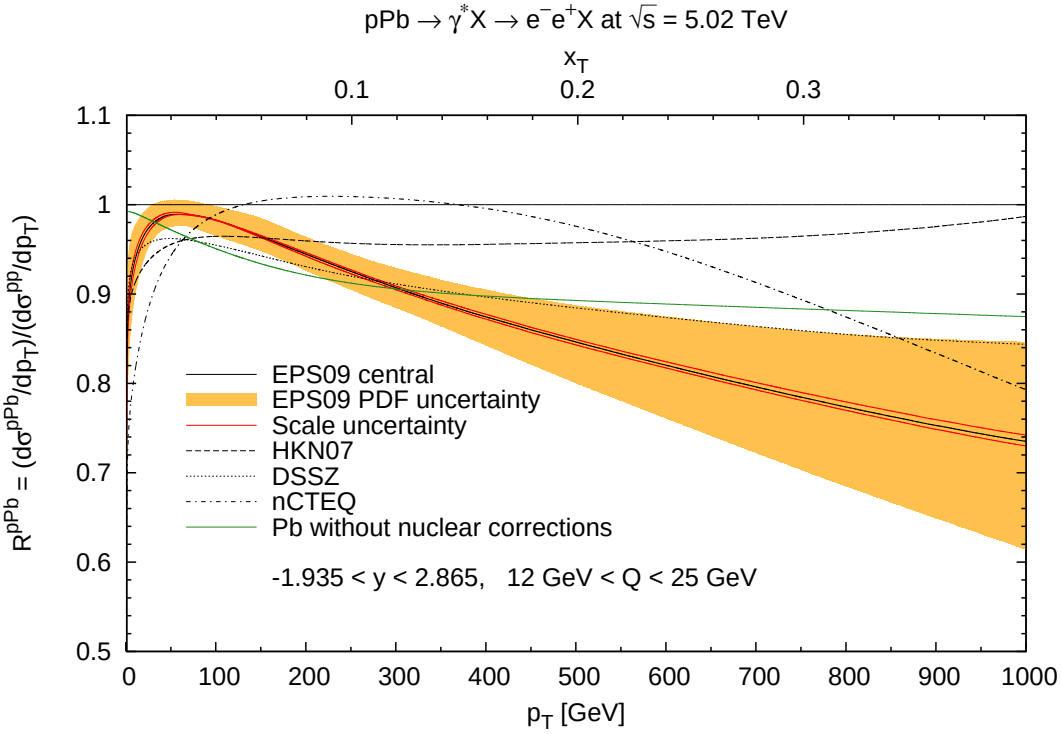

Figure 8. Same as Fig. 6 for slightly larger dilepton invariant mass and considerably larger transverse momenta.

measurements could be reliably used to constrain the nuclear PDFs. nCTEQ predict again much stronger shadowing of more than 32%, contrary to 14% for EPS09, 12% for HKN07 and even only 6% for DSSZ.

If the proton and lead beam directions are reversed, the situation changes dramatically, as can be seen from Fig. 7 (bottom). The ALICE forward muon spectrometer is now mostly probing bound valence quarks, so that all parametrisations are following to first approximation the prediction from isospin effects only (green). Furthermore, the central EPS09 curve predicts antishadowing up to p_T of about 40 GeV and an EMC effect beyond this value. The other parametrisations see this transition only at the high end of the p_T-range shown here, i.e. at 70, 90 and 95 GeV for DSSZ, HKN07 and nCTEQ, respectively. They fall outside the EPS09 uncertainty band, which is quite small ($\pm 2\%$), over almost the entire p_T-range, differing from it by up to 8%. Scale uncertainties are again very small, so that the LHC measurements proposed here can be of great importance not only in the small-, but also in the large-x regions.

With the central detectors of ATLAS and CMS, it should be possible to measure electron-positron and muon pairs with slightly larger invariant mass and considerably larger transverse momenta than in the ALICE experiment, but nevertheless providing again access to the regions with antishadowing, isospin and EMC effects as with the ALICE forward muon spectrometer. This is confirmed by Fig. 8, which is qualitatively similar to the Fig. 7 (bottom). Isospin effects soon take the leading role. According to the EPS09 and DSSZ

predictions, the transition from antishadowing to the EMC effect should happen at 300 GeV. Below (above) this value, the DSSZ prediction has larger antishadowing and smaller EMC effects and lies close to or at the edge of the EPS09 uncertainty band. The shapes of HKN07 and nCTEQ are very different, which can be attributed to smaller/older data sets and a more general parametrisation of nuclear effects, respectively. With nCTEQ in particular, the transition to the EMC effect region occurs only at very large p_T. A similar behavior had already been observed in Fig. 7 (bottom).

5 Conclusions

In conclusion, we have proposed in this paper measurements of low-mass lepton pair production in proton-lead collisions at the LHC to better constrain the nuclear parton densities. After reminding the reader about our currently very unsatisfactory knowledge of nuclear corrections, in particular for the gluon at small x, but also for other partons at large x, we established the dominance of quark-gluon scattering in analogy with real photon production, but without its theoretical and experimental fragmentation and isolation uncertainties. Using NLO QCD calculations and current experimental acceptances of electrons and muons in the ALICE, ATLAS and CMS experiments, we numerically demonstrated that measuring ratios of transverse momentum distributions has a large potential to reduce the theoretical uncertainties on the nuclear modifications of PDFs or even rule out some parametrisations. Depending on beam orientation and central or forward kinematics, all interesting regions, shadowing, antishadowing, isospin and effects can be probed, while scale and bare-proton PDF uncertainties, as well as many systematic experimental errors, should cancel out. The results of these measurements could subsequently be used to establish new, more reliable nuclear PDFs in global fits.

Acknowledgments

We thank C. Klein-Bösing for useful discussions and comments on the manuscript.

References

[1] M. Wilde [ALICE Collaboration], Nucl. Phys. A904-905 **2013** (2013) 573c [arXiv:1210.5958 [hep-ex]].

[2] M. Klasen, C. Klein-Bösing, F. König and J. P. Wessels, arXiv:1307.7034 [hep-ph].

[3] M. Hirai, S. Kumano and T. -H. Nagai, Phys. Rev. C **76** (2007) 065207 [arXiv:0709.3038 [hep-ph]].

[4] I. Schienbein, J. Y. Yu, K. Kovarik, C. Keppel, J. G. Morfin, F. Olness and J. F. Owens, Phys. Rev. D **80** (2009) 094004 [arXiv:0907.2357 [hep-ph]].

[5] K. J. Eskola, H. Paukkunen and C. A. Salgado, JHEP **0904** (2009) 065 [arXiv:0902.4154 [hep-ph]].

[6] D. de Florian, R. Sassot, P. Zurita and M. Stratmann, Phys. Rev. D **85** (2012) 074028 [arXiv:1112.6324 [hep-ph]].

[7] N. Hammon, A. Dumitru, H. Stoecker and W. Greiner, Phys. Rev. C **57** (1998) 3292 [hep-ph/9801292].

[8] F. Arleo and T. Gousset, Phys. Lett. B **660** (2008) 181 [arXiv:0707.2944 [hep-ph]].

[9] F. Arleo, K. J. Eskola, H. Paukkunen and C. A. Salgado, JHEP **1104** (2011) 055 [arXiv:1103.1471 [hep-ph]].

[10] S. Catani, M. Fontannaz, J. P. .Guillet and E. Pilon, JHEP **1309** (2013) 007 [arXiv:1306.6498 [hep-ph]].

[11] L. Bourhis, M. Fontannaz and J. P. Guillet, Eur. Phys. J. C **2** (1998) 529 [hep-ph/9704447].

[12] E. L. Berger, L. E. Gordon and M. Klasen, Phys. Rev. D **58** (1998) 074012 [hep-ph/9803387].

[13] E. L. Berger, L. E. Gordon and M. Klasen, Phys. Rev. D **62** (2000) 014014 [hep-ph/9909446].

[14] M. Brandt and M. Klasen, arXiv:1305.5677 [hep-ph].

[15] Z. -B. Kang and J. -W. Qiu, Phys. Lett. B **721** (2013) 277 [arXiv:1212.6541].

[16] V. Guzey, M. Guzzi, P. M. Nadolsky, M. Strikman and B. Wang, Eur. Phys. J. A **49** (2013) 35 [Eur. Phys. J. A **49** (2013) 35] [arXiv:1212.5344 [hep-ph]].

[17] D. Stump, J. Huston, J. Pumplin, W. -K. Tung, H. L. Lai, S. Kuhlmann and J. F. Owens, JHEP **0310** (2003) 046 [hep-ph/0303013].

[18] A. D. Martin, R. G. Roberts, W. J. Stirling and R. S. Thorne, Eur. Phys. J. C **4** (1998) 463 [hep-ph/9803445].

[19] A. D. Martin, W. J. Stirling, R. S. Thorne and G. Watt, Eur. Phys. J. C **63** (2009) 189 [arXiv:0901.0002 [hep-ph]].

[20] J. Pumplin, D. R. Stump, J. Huston, H. L. Lai, P. M. Nadolsky and W. K. Tung, JHEP **0207** (2002) 012 [hep-ph/0201195].

[21] CMS Collaboration [CMS Collaboration], CMS-PAS-HIN-12-017.

[22] T. Ince, talk given at the ATLAS editorial board meeting, January 2012;
J. Goddard, talk given at the IOP 2013 HEPP and APP Group Meeting, Liverpool, `https://indico.cern.ch/conferenceDisplay.py?confId=214998`.

[23] C. Baumann [ALICE Collaboration], EPJ Web Conf. **36** (2012) 00003 [arXiv:1210.2772 [nucl-ex]].

[24] R. Arnaldi [ALICE Collaboration], Nucl. Phys. A **904-905** (2013) 595c [arXiv:1211.2578 [nucl-ex]].

[25] B. B. Abelev *et al.* [ALICE Collaboration], arXiv:1308.6726 [nucl-ex].

[26] G. Aad *et al.* [ATLAS Collaboration], Phys. Lett. B **720** (2013) 32 [arXiv:1211.6899 [hep-ex]].

[27] S. Chatrchyan *et al.* [CMS Collaboration], JHEP **1312** (2013) 030 [arXiv:1310.7291 [hep-ex]].